Polymer Chemistry

ROYAL SOCIETY
OF **CHEMISTRY**

PAPER
Robert B. Moore *et al.*
Blocky bromination of syndiotactic polystyrene *via* post-polymerization
functionalization in the heterogeneous gel state

Check for updates

Blocky bromination of syndiotactic polystyrene *via* post-polymerization functionalization in the heterogeneous gel state†

Kristen F. Noble, [ID] [a] Alexandria M. Noble, [ID] [b] Samantha J. Talley [ID] [a] and Robert B. Moore [ID] *[a]

This work demonstrates the successful blocky bromination of syndiotactic polystyrene (sPS-*co*-sPS-Br) copolymers containing 6–30 mol% *p*-bromostyrene units, using a post-polymerization functionalization method conducted in the heterogeneous gel state. For comparison, a matched set of randomly brominated sPS-*co*-sPS-Br copolymers was prepared using homogeneous (solution-state) reaction conditions. The degree of bromination and copolymer microstructure were evaluated using ^{1}H and ^{13}C nuclear magnetic resonance (NMR) spectroscopy. The NMR spectra of gel-state (Blocky) and solution-state (Random) copolymers exhibit strikingly different resonance frequencies and peak intensities above 6 mol% Br and provide direct evidence that functionalization in the gel state produces copolymers with non-random "blocky" microstructures. Quenched films of the Blocky copolymers, analyzed using ultra-small-angle X-ray scattering (USAXS) and small-angle X-ray scattering (SAXS), show micro-phase separated morphologies, which further supports that the Blocky copolymers contain distinct segments of pure sPS and segments of randomly brominated sPS unlike their completely Random analogs. Crystallization behavior of the copolymers, examined using differential scanning calorimetry (DSC), demonstrates that the Blocky copolymers are more crystallizable and crystallize faster at lower supercooling compared to their Random analogs. Computer simulations of the blocky copolymers were developed based on the semicrystalline morphology of a 10 w/v% sPS/CCl$_4$ gel, to rationalize the effect of heterogeneous functionalization on copolymer microstructure and crystallization behavior. The simulations were found to agree with the microstructural analysis based on the NMR results and confirm that restricting the accessibility of the brominating reagent to monomers well removed from the crystalline fraction of the gel network produces copolymers with a greater prevalence of long, uninterrupted sPS homopolymer sequences. Thus, the blocky microstructure is advantageous for preserving desired crystallizability of the resulting blocky copolymers.

Introduction

Block copolymers are a class of macromolecules, characterized by two or more chemically distinct polymer segments linked together through covalent bonds.[1,2] The individual characteristics of the discrete block segments, for example the chemical nature of the repeating monomers, block lengths and distribution, number of blocks, and chain architectures, govern the chemical and physical properties of the block copolymer.

Moreover, the thermodynamic immiscibility between chemically dissimilar blocks often drives self-assembly into well-ordered, micro-phase separated morphologies that can significantly enhance the material properties. The technological applicability of block copolymers is promising; however, the generally arduous procedures for block copolymer synthesis, often involving inert atmospheric conditions, well-controlled, sequential reaction timings, specialized initiators, and high purity monomers and solvents, generally limits the scope of their commercial application. To achieve crystallizable block copolymers, stereo/regiocontrolled living polymerization mechanisms are generally necessary, which presents an additional challenge that often requires the development of system-specific catalysts and significant synthetic skill.[3]

As a distinct alternative to the complex polymerization mechanisms and synthetic protocols employed in the conven-

[a]Department of Chemistry and Macromolecules Innovation Institute, Virginia Tech, Blacksburg, VA 24061, USA. E-mail: rbmoore3@vt.edu
[b]Grado Department of Industrial and Systems Engineering, Virginia Tech, Blacksburg, VA 24061, USA
†Electronic supplementary information (ESI) available. See DOI: 10.1039/c8py01008k

tional formation of block copolymers, our recent efforts have demonstrated that blocky copolymer microstructures can be achieved using comparatively simple post-polymerization functionalization chemistries carried out on semicrystalline homopolymers in their heterogeneous gel state.[4,5] Herein, the term "blocky copolymer" will be used as a description of gel-state functionalized copolymers, implying a significant degree of non-randomness in the distribution of comonomers along the copolymer chain.

Gels of crystallizable homopolymers (*e.g.*, sPS) are composed of tightly packed chain segments in lamellar crystallites that act as physical cross-links bound together by a percolating network of solvent swollen amorphous chains.[6–10] When a functionalizing reagent is introduced to the heterogeneous gel network, it is sterically excluded from the crystalline component, and thus only reacts with monomer units in the accessible interconnecting amorphous component. Using this straightforward post-polymerization functionalization approach, the resulting copolymer is likely to contain separate segments of randomly functionalized "blocks" and un-functionalized "blocks" originating from monomer units that were isolated within the crystalline domains of the gel. By controlling the precise morphology of the semicrystalline gel, specifically the crystallite dimensions and degree of crystallinity, distinct blocks of highly functionalized segments with tunable sequence distributions and chemical compositions are anticipated.

Heterogeneous functionalization reaction schemes reported in the literature set a precedent for utilizing gel-state reaction conditions to produce copolymers with blocky microstructures. For example, we recently demonstrated that the heterogeneous sulfonation of sPS[4] and poly(ether ether ketone)[5] (PEEK) gels,

yields ionomers with a blocky distribution of functionalities along the chains. The gel-state sulfonated sPS and PEEK ionomers demonstrated superior crystallizability and faster crystallization kinetics compared to their solution-state sulfonated random analogs, consistent with copolymers with blocky microstructures. Similarly, Venditto and coworkers[11] showed that exposing a gel of semicrystalline syndiotactic polystyrene (sPS) to chlorosulfonic acid results in preferential sulfonation of the gel's amorphous component. While evidence of a blocky microstructure was not directly explored, their heterogeneous method is effectively equivalent to our gel-state sulfonation approach[4,12,13] to produce blocky copolymers. In earlier work, Borriello and coworkers[14] investigated the post-polymerization sulfonation of solution cast or compression-molded sPS films, evaluating the interplay between sulfonating reagent diffusion and reaction processes on sulfonation heterogeneity across the films. Solution cast films demonstrated uniform sulfonation, attributed to rapid diffusion of sulfonating reagent through nanoporous phases in the film. In contrast, compression-molded films exhibited a decreasing sulfonation gradient from the film's surface to interior, consistent with slow diffusion of sulfonating reagent into the non-porous, solid-state "bulk" film. This result is also similar to that observed for the sulfonation of atactic polystyrene (aPS) films.[15] Genzer and coworkers[16–21] used experimental and theoretical results to extensively investigate the bromination of aPS in poor solvents, where polymer chains are in a collapsed conformation. In this collapsed state, portions of the chains were effectively shielded from the brominating reagent, resulting in blocky brominated styrene sequences. Others have performed post-polymerization bromination[22] or acetylation[23] on suspended sPS powders, though copolymer microstructure was not investigated in these
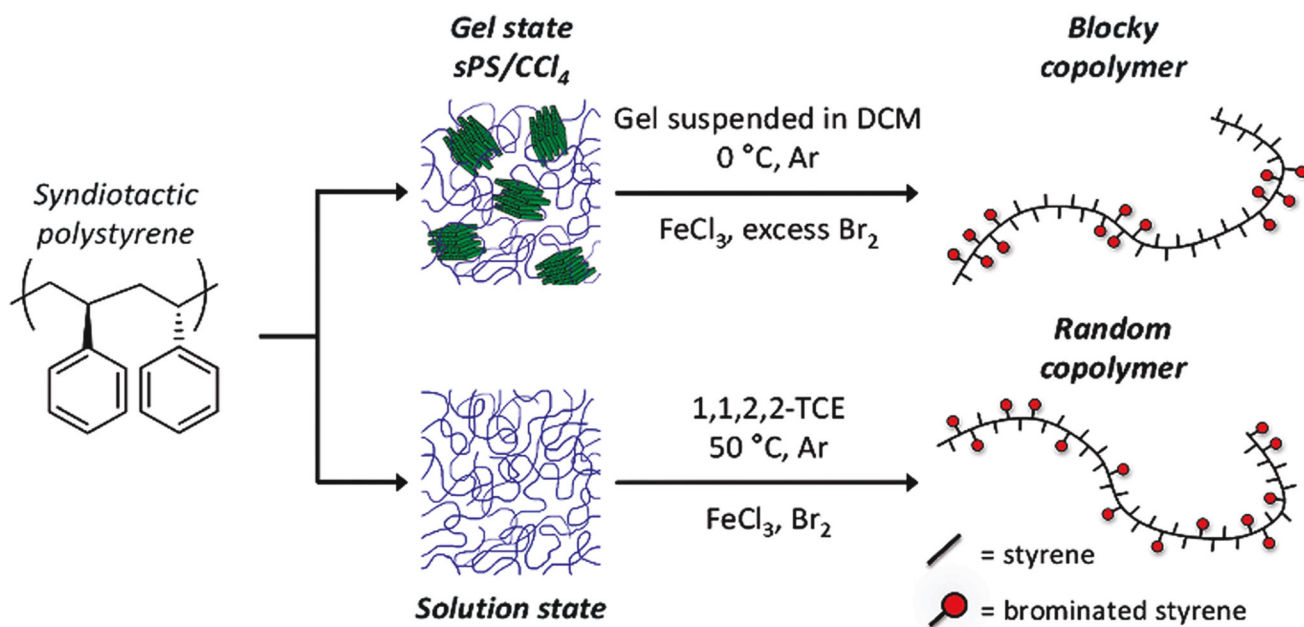
Scheme 1 Schematic representation of sPS bromination *via* post-polymerization functionalization in solution and in the heterogeneous gel state.

studies. Ultimately, to produce sPS-based copolymers that retain crystallizability of the sPS component with the added advantage of distinct properties attributed to the functional component, block or blocky copolymer microstructures are required.[24–26]

This work reports the first post-polymerization bromination of sPS in solution and in the heterogeneous gel-state to produce a matched set of random and blocky brominated sPS (sPS-*co*-sPS-Br) copolymers (Scheme 1). The purpose of this research was to prepare *semicrystalline* blocky copolymers with relatively high degrees of functionality using a facile, post-polymerization functionalization method. To investigate how the specific distribution of functional groups along the chains effects copolymer properties, NMR spectroscopy was used to evaluate the copolymer microstructure, X-ray scattering techniques were used to investigate the copolymer film morphology, and differential scanning calorimetry (DSC) was used to probe the crystallizability and crystallization kinetics of the copolymers. In order to obtain further insight into the effect of gel-state bromination on copolymer microstructure and to rationalize the effect of copolymer microstructure on the observed crystallization behavior, computer simulations of the random and blocky copolymers have been developed. Through this work, post-polymerization functionalization carried out in the gel state is proven to be a facile approach to prepare semi-crystalline sPS-*co*-sPS-Br copolymers with blocky microstructures and tunable crystallization properties. Given a wealth of aromatic Br substitution chemistries,[27–29] the broader scope of this work is to use these blocky brominated sPS copolymers as templates to produce new functional materials with desirable physical and chemical properties that originate from the easily obtained blocky microstructure.

Experimental section

Materials

Syndiotactic polystyrene (Questra® 102) of 300 000 g mol^{-1} weight average molecular weight (M_w) was obtained from Dow Chemical Company. Carbon tetrachloride (CCl_4), 1,1,2,2-tetrachloroethane (TCE), and 1,2-dichloromethane (DCM) were purchased from Fischer Scientific Company. Bromine (Br_2) was obtained from Sigma Aldrich®. The Lewis acid catalyst, ferric(III) chloride ($FeCl_3$), was purchased from VWR International LLC. All chemicals and reagents were used as received.

Gel-state bromination to produce blocky copolymers

To prepare the gel, sPS (2.5 g, 0.83 μmol) pellets were first dissolved in CCl_4 (25 mL) in a pressure vessel at 120 °C, then removed from heat to promote gel formation. The gel formed within a period of one hour and was stored at room temperature for *ca.* 24 h prior to use. Using a spatula, the gel was broken into small pieces (*ca.* 1–3 mm), transferred to a round bottom flask and dispersed in DCM (final sPS concentration of 3 w/v%). After addition of $FeCl_3$ (68 mg, 0.42 mmol), the

flask was placed in an ice bath and purged with argon for 30 min. To brominate the sPS gel, a stock solution of 50 w/w% Br_2 in DCM (4.3 mL Br_2, 0.084 mol) was added dropwise to the reaction vessel over two hours. In order to minimize bromination of the backbone by bromine radicals (Br$^{\cdot}$), the reaction was carried out in the dark under argon at room temperature.[27] To control the degree of bromination, reactions were halted after 6, 18, 24, or 51 hours by pouring the suspensions into stirred methanol. All samples were purified by dissolving in TCE, filtering, and precipitating in methanol to recover a white product. Prior to analysis, samples were ground into homogenous powders, washed by soxhlet extraction in hot methanol for *ca.* 24 h, and dried under vacuum at 110 °C for *ca.* 18 h.

Bromination in the solution-state to produce random copolymers

To prepare the solution, sPS pellets (2.0 g, 0.67 μmol) were dissolved in TCE (25 mL) at 130 °C. The solution temperature was lowered to 50 °C, $FeCl_3$ (5 mol% based on the amount of Br_2) was added, and the solution was purged with argon for *ca.* 30 min. Bromine stock solution was added dropwise and the reaction was allowed to proceed for 2 h in the dark under argon at a final sPS concentration of 1 w/v%. To control the degree of bromination, reactions were carried out using mol ratios of Br_2 to styrene monomer of 0.10 : 1, 0.30 : 1, 0.40 : 1, or 0.70 : 1. Reaction solutions were poured into stirring methanol, filtered, washed, and dried to yield an off-white product. Samples were purified by dissolving in TCE and precipitating in methanol. All samples were homogenized by grinding, washed by soxhlet extraction in hot methanol for *ca.* 24 h, and dried under vacuum at 110 °C for *ca.* 18 h.

NMR spectroscopy

Microstructure analysis was carried out using nuclear magnetic resonance (NMR) spectroscopy. ^{1}H NMR, [1]H–[13]C heteronuclear single quantum coherence (gHSQC), and [1]H–[13]C band-selective heteronuclear multiple bond correlation (bsgHMBC) experiments were recorded at room temperature in CDCl$_3$ or TCE-d$_2$ on an Agilent U4-DD2 400 MHz spectrometer. Quantitative ^{13}C NMR experiments were recorded at room temperature in TCE-d$_2$ on a Bruker Avance II 500 MHz spectrometer (C13IG parameter set, proton decoupled, relaxation delay of 6 s, O1P of 95, and sweep width of 150 ppm). Determination of the degree of bromination (mol% Br) from the ^{1}H NMR spectrum is described in the Results and discussion section.

Thermal properties and crystallization kinetics

Copolymer thermal transitions and crystallization kinetics were probed using differential scanning calorimetry (DSC, TA Instruments DSC Q2000) under continuous nitrogen flow to minimize polymer degradation. To investigate crystallizability under specific cooling conditions, samples were first annealed at 300 °C for 3 min to erase thermal history, then cooled to 0 °C at −60 °C min^{-1} (rapid cool) or −10 °C min^{-1} (slow cool). Isothermal crystallization from the melt (300 °C held for 5 min and cooled at −60 °C min^{-1}) was carried out at 190 °C for 2 h.

All heating scans were recorded at 10 °C min^{-1}. TA Instruments Universal Analysis software was used to determine glass transition temperatures (T_g), crystallization temperatures at maximum exothermic heat flow (T_c), and melting temperatures at maximum endothermic heat flow (T_m). To ascertain crystallization half-times ($t_{1/2}$), defined as the time at which a material attains 50% of its maximum crystallinity, samples were subjected to isothermal crystallization at specific crystallization temperatures below T_m. The isothermal crystallization profiles (heat flow versus time) were analyzed using the following approach:

$$F_c(t) = \frac{\int_0^t \frac{dH}{dt}\,dt}{\int_0^\infty \frac{dH}{dt}\,dt} \qquad (1)$$

where $F_c(t)$ is the bulk fractional crystallinity of the functionalized copolymer systems, equal to the heat evolved during isothermal crystallization at a specific time t divided by the total heat evolved during the isothermal crystallization process. The resulting crystallization isotherms (F_c versus time) were used to determine $t_{1/2}$ by extrapolating F_c at 0.5 to the time axis, and these $t_{1/2}$ values were used as a comparative measure of the overall rate of bulk crystallization.

Ultra-small-angle and small-angle X-ray scattering

Films were prepared from powders of the sPS homopolymer and Random and Blocky copolymers by melt pressing between Kapton sheets at 30 °C above T_m for 20 s at 2200 psi then for 20 s at 4500 psi, followed by quenching in ice water to prevent sPS crystallization. Ultra-small-angle X-ray scattering (USAXS) and small-angle X-ray scattering (SAXS) experiments were performed at the Advanced Photon Source beamline 9ID-C at Argonne National Laboratory.[30–32] The USAXS instrument was configured in standard mode with an X-ray energy of 21 keV (λ = 0.5895 Å), X-ray photon flux of ca. 1013 mm^{-2} s^{-1}, and a combined q range of 0.0001–1.3 Å^{-1} ($q = 4\pi/\lambda \sin(\theta)$, where λ is the wavelength and θ is one-half of the scattering angle). The USAXS and SAXS profiles were acquired sequentially and merged into a single data set using the Irena SAS package.[33] The observed scattering features in the desmeared USAXS/SAXS profiles were analyzed using the Unified Fit, described in the Irena tool suite.[33]

Wide-angle X-ray diffraction

Wide-angle X-ray diffraction (WAXD) experiments were performed using a Rigaku MiniFlex II X-ray diffractometer emitting X-rays with a wavelength of 0.154 nm (Cu K$_\alpha$). Samples were scanned from 5° to 35° 2θ at a scan rate of 0.250° 2θ min^{-1} and a sampling window of 0.050° 2θ at a potential of 30 kV and current of 15 mA. All WAXD data were analyzed using the PDXL 2 software package to obtain WAXD intensity versus 2θ profiles.

Simulations of random and blocky copolymer microstructures

Representative chain microstructures resulting from the homogeneous and heterogeneous reaction states for sPS bromina-tion were simulated using a code created with MATLAB® R2017a programming software (the code used for these simulations is provided in the ESI†). For each degree of functionalization, the MATLAB® code simulates 1000 homopolymer chains of 1442 monomer units (based on our sPS sample, M_w = 300 K; $Đ$ = 2.0). To simulate the random microstructure resulting from homogeneous solution-state functionalization, monomers along the chain are selected at random up to the desired degree of bromination. To simulate the blocky microstructure resulting from functionalization in the semicrystalline gel state, an inaccessible fraction of monomers, representing crystalline chain segments in the physical gel, was first established prior to random bromination of the remaining accessible fraction, representing the amorphous chain segments of the gel. The rationalization for the specific inaccessible fraction of monomers used in these simulations is based on the measured degree of crystallinity in a 10 w/v% sPS/CCl$_4$ gel and is discussed in more detail below in the Results and discussion section. For each simulated polymer chain, the length and frequency of consecutive styrene (S) and Br-styrene (B) units, and the prevalence of each unique triad sequence (e.g., SSS, BBB, etc.) is calculated.

Results and discussion

Microstructure analysis using NMR spectroscopy

To investigate the sPS-co-sPS-Br copolymer microstructure, gel-state (Blocky, B-x%) and solution-state (Random, R-x%) copolymers were prepared in a matched set of approximately x = 6, 15, 20, and 30 mol% brominated styrene (Br-Sty) units and analyzed by NMR spectroscopy. Fig. 1 shows the aromatic region of the ^{1}H NMR spectra of the Random and Blocky copolymers (for full spectra, see Fig. S1†). Compared to pure sPS,
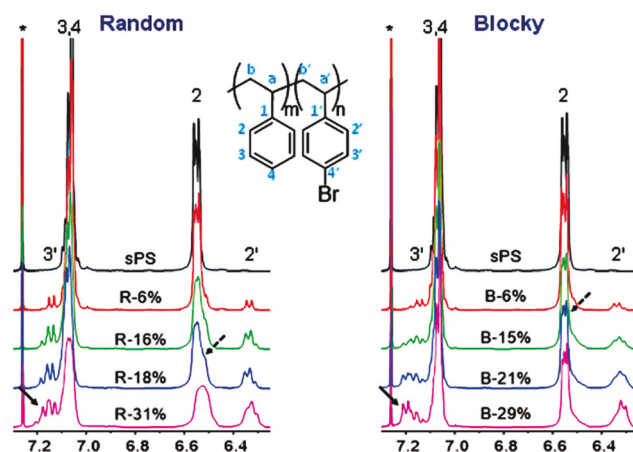

Fig. 1 Aromatic region of the ^{1}H NMR spectra of (left) solution-state Random and (right) gel-state Blocky copolymers increasing in mol% Br from top to bottom. For comparison, spectra are referenced to CDCl$_3$ and normalized over 6.27–6.60 ppm. The asterisk (*) indicates solvent resonance. The arrows highlight differences between spectra.

new proton resonances appear in the ^{1}H NMR spectrum of the sPS-*co*-sPS-Br copolymers at 1.23, 1.58–1.75, 6.27–6.38, and 7.11–7.22 ppm, corresponding to the methylene (H(b′)) and methine (H(a′)) protons, and the aromatic protons (H(2′) and H(3′)) of Br-Sty monomers, respectively. Resonance assignments were verified by homonuclear and heteronuclear two-dimensional (2D) NMR experiments included in Fig. S3 and 4.† To verify the absence of backbone bromination, the total peak areas of the methylene (H(b), H(b′)) and methine (H(a), H(a′)) group resonances for brominated and un-brominated monomers were compared and found to be consistent with the expected 2 : 1 ratio. The mol% Br was derived from the fraction of *ortho*-proton resonances of Br-Sty monomers (H(2′), 6.27–6.38 ppm) to the total area of styrene (H(2)) and Br-Sty *ortho*-proton resonances (6.27–6.60 ppm). Notably, the degree of bromination increased with increasing mol ratio of Br$_2$ to styrene monomer when the polymer was dissolved in solution and increasing reaction time in the presence of homopolymer gel, validating that the reaction methods effectively control the degree of functionalization.

Comparing the ^{1}H NMR spectra of Random and Blocky copolymers reveals significant differences in their peak intensities and proton chemical shifts, despite their similar Br-contents. For the Random copolymers, resonances attributed to un-brominated styrene units (*e.g.*, H(2) and H(3,4)) broaden with increasing functionalization, consistent with a decrease in the sequence length of pure homopolymer segments (dashed arrows in Fig. 1). In contrast, the Blocky copolymers exhibit sharp proton resonances similar to that of pure sPS even at high mol% Br. This behavior suggests that the Blocky copolymers contain a greater fraction of uninterrupted sPS segments compared to their Random analogs. In addition, the H(3′) proton resonances of Blocky Br-Sty units appear to shift downfield with increasing degree of functionalization, indicated by the solid arrows in Fig. 1. The high frequencies and strong intensities of the H(3′) resonances in Blocky B-21% and B-29% are consistent with an accumulation of neighboring electronegative *p*-bromostyrene units, a strong indicator that these copolymers have numerous dyads and triad sequences of Br-Sty monomers. Notably, the shape of the H(3′) peak in B-29% is also consistent with that observed for a highly brominated (59 mol% Br) sPS-*co*-sPS-Br copolymer prepared *via* copolymerization by Guo and co-workers.[34] Overall, the microstructural information provided by ^{1}H NMR yields strong evidence that gel-state bromination produces copolymers with long segments of consecutive styrene units and segments of densely brominated sPS, characteristic of a blocky copolymer microstructure.

Quantitative ^{13}C NMR spectroscopy was used to provide a deeper insight into the microstructure of the Random and Blocky copolymers. Fig. 2 shows the aromatic carbon spectral region of the sPS homopolymer and sPS-*co*-sPS-Br copolymers (for full spectra, see Fig. S2†). Upon *para*-substitution of the phenyl rings with bromine, new carbon resonances appear in the ^{13}C NMR spectrum. The new resonances at 40.0 and 43.6 ppm are attributed, respectively, to the methine (C(a′))

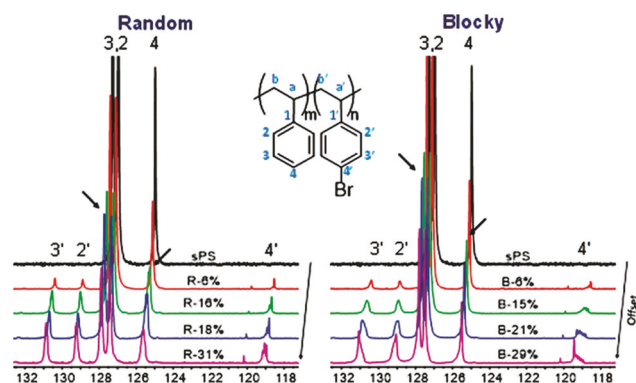**Fig. 2** Aromatic C(2–4) and C(2′–4′) resonances in the ^{13}C NMR spectra of the (left) Random and (right) Blocky copolymers increasing in mol% Br from top to bottom. For comparison, spectra are referenced to TCE-d$_2$ and normalized over 127.0–132.5 ppm.

and methylene (C(b′)) carbons of Br-Sty monomers. The resonances at 129.2 and 130.9 ppm are assigned, respectively, to the *ortho*-(C(2′)) and *meta*-carbons (C(3′)) of brominated phenyl rings. Multiple peaks are observed between 118.8–119.3 and 142.9–144.9 ppm, attributed to the Br-substituted phenyl carbons (C–Br, C(4′)) and the quaternary phenyl carbons of brominated (C(1′)) and un-brominated (C(1)) monomers, respectively. Throughout the Blocky copolymer series, carbon resonances of un-brominated styrene monomers are sharp and intense compared to their Random analogs, indicated by arrows in Fig. 2. Similar to the behavior observed in the ^{1}H spectra above, this further suggests that the blocky copolymer microstructure is comprised of long segments of pure sPS, even at high Br-contents.

Chemical shifts in ^{13}C NMR spectra are highly dependent on the electronic environments of the carbon nuclei, which can be used to evaluate comonomer sequence distribution and provide insight into the short-range microstructure of a copolymer.[35,36] For the sPS-*co*-sPS-Br copolymers, the C(4′) resonance appears to be sensitive to copolymer microstructure, demonstrated by the appearance of multiple peaks in the ^{13}C NMR spectra of the Random and Blocky samples with increasing mol% Br (Fig. 2). The C(4′) region of Blocky B-29% exhibits five distinct peaks. The sharp C(4′) peak at 119.4 ppm in Blocky B-29% does not appear in the spectrum of Random R-31%, but is consistent with the chemical shift of C(4′) observed in sPBrS homopolymers.[34] Thus, this peak is characteristic of a copolymer with long segments of consecutive Br-Sty units. Interestingly, prior to this research, only chemical shifts of the backbone and C(1) carbons of polystyrene and poly(styrene-*co*-bromostyrene) copolymers were thought to be sensitive to copolymer microstructure.[35] Due to complexities arising from stereoirregularity, attempts by others to evaluate copolymer "blockiness" and comonomer sequence distribution in halogenated[21,36,37] and sulfonated[38,39] *atactic* polystyrene-based copolymers by NMR have been generally unsuccessful.[35,39,40] However, with the high tactic purity of *syndiotactic* polystyrene, this work further demonstrates that ^{13}C NMR

spectroscopy can be used to evaluate comonomer sequence distribution.[41,42]

The most profound evidence for microstructural differences between the Random and Blocky copolymers is observed by comparing the quaternary C(1) and C(1′) carbon spectra, shown in Fig. 3. For the Random samples, bromination of sPS produces multiple new peaks that increase in intensity with increasing Br-content. The multiple peaks signify through-bond communication between neighboring brominated and un-brominated styrene monomers, and likely provide a unique fingerprint of the copolymer microstructure originating from the specific comonomer sequence distribution. For the Blocky samples, the quaternary carbon peak distributions and intensities differ strikingly from their Random analogs at all degrees of bromination, which is emphasized by the new resonance in Blocky B-21% and B-29% at 143.1–143.3 ppm. Based on the C(1′) chemical shift of the sPBrS homopolymer[34] which occurs at 143.1 ppm, our assignment of this new peak is to a Br-Sty triad (BBB). By integrating this peak relative to the full range of the C(1) and C(1′) resonances, the prevalence of the BBB triad in Blocky B-29% is found to be approximately 17%. This high prevalence for the Blocky sample is remarkable given that the quaternary carbon spectrum of Random R-31% does not exhibit a distinct peak at 143.1–143.3 ppm, demonstrating that random bromination results in a relatively low abundance of BBB triad. Our efforts to assign the remaining quaternary carbon peaks in the Random and Blocky copolymers to triad and pentad sequences and with comparison to simulations of random and blocky copolymer microstructures will be thoroughly discussed in a subsequent publication. In summary, our initial microstructural analysis using NMR spectroscopy proves that the bromination method can be used to manipulate copolymer sequence; solution-state bromination produces random copolymers while gel-state bromination clearly produces sPS-co-sPS-Br copolymers with blocky microstructures.
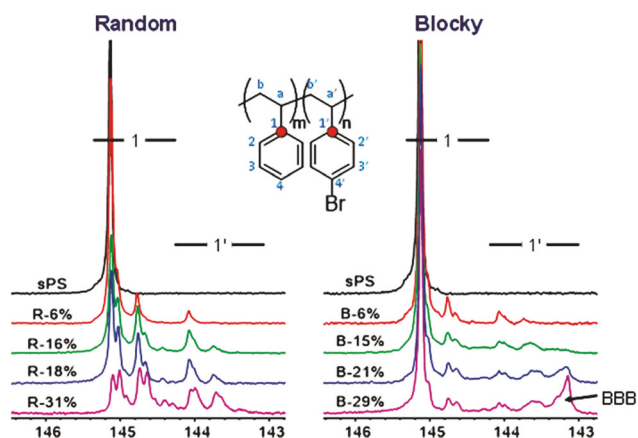

Fig. 3 C(1) and C(1′) NMR spectra of the (left) Random and (right) Blocky copolymers increasing in mol% Br from top to bottom. For comparison, spectra are referenced to TCE-d$_2$ and normalized over 127.0–132.5 ppm.

Thermal transitions

DSC thermograms of the sPS homopolymer and the Random and Blocky copolymers after rapid cooling from the melt to 0 °C at −60 °C min^{-1} are shown in Fig. 4. The heating trace of pure sPS displays two endothermic events, the glass transition at 98 °C and an intense melting endotherm at 272 °C. At approximately 6 mol% Br, both the Random and Blocky copolymers crystallize during cooling and exhibit similar depression in their melting temperatures, T_m, relative to pure sPS. Bromine groups attached to a crystallizable polymer can act as physical defects along the polymer chains, limiting crystallizability and lamellar thickness. It is not surprising then that both copolymer series show a depression in T_m with increasing Br-content as a consequence of shorter crystallizable chain segments and thus thinner crystallites.[23,26,27,43] Nonetheless, it is important to note that the melting point depression for the Random copolymers occurs to a much greater extent compared to the Blocky copolymers, despite their analogous Br-contents (see Fig. S5†).

Above 6 mol% Br, the Blocky copolymers show an exothermic event observed between 150–200 °C (Fig. 4), ascribed to cold crystallization during heating. Cold crystallization during the heating scan following a rapid cool is attributed to a reduction in the rate of crystallization.[23,26] During conditions of slow cooling (−10 °C min^{-1}), the crystallization exotherm, T_c, decreases in temperature and intensity with increasing Br-content, which also reflects a reduction in the rate of crystallization (see Fig. S6†). In distinct contrast to the behavior of the Blocky samples, the 18 mol% Br and above Random samples do not crystallize under the thermal conditions of this experiment. This behavior demonstrates that the Blocky samples are much more crystallizable throughout the copolymer series. Remarkably, the Blocky B-29%, which has approximately one Br-Sty for every three styrene monomers, is still crystallizable and exhibits a melting endotherm at 216 °C. This result strongly implies a blocky distribution of Br-Sty units along the copolymer chains.

To further examine the effect of blocky versus random microstructure on crystallizability, the weight percent crystallinity (%X_c) was calculated from the area under the melting endotherm (ΔH_f) with respect to the heat of fusion of 100% crystalline pure sPS[44] ($\Delta H_f^\circ = 82.6 \, J \, g^{-1}$). Table 1 summarizes
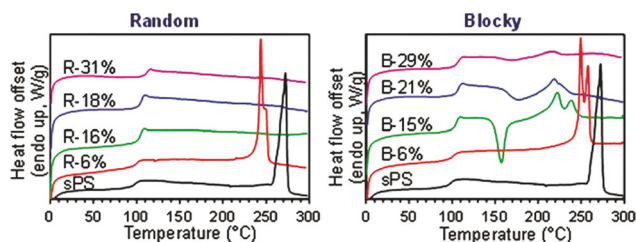

Fig. 4 DSC heating scans of the sPS homopolymer and the (left) Random and (right) Blocky copolymers after rapid cooling from the melt (300 °C) at −60 °C min^{-1}. Heating rate: 10 °C min^{-1}.

Table 1 Thermal properties and weight percent crystallinity of the sPS homopolymer and the Random and Blocky copolymers measured using DSC

Sample	After slow cooling at −10 °C min⁻¹				After 2 h isothermal crystallization at 190 °C	
	T_g (°C)	T_m (°C)	T_c^a (°C)	X_c (%)	T_m (°C)	X_c (%)
sPS	100	270	237	31	270	31
B-6%	102	249	215	24	249	28
B-15%	106	234	187	17	234	21
B-21%	105	222	180	16	222	18
B-29%	107	213	—	4	218	5
R-6%	100	245	204	23	245	28
R-11%	96	227	175	25	230	27
R-16%	105	215	—	<1	216	18
R-18%	106	—	—	0	213	<1
R-31%	111	—	—	0	—	0

T_g = glass transition temperature; T_m = temperature at maximum endothermic heat flow. ^{a} T_c = temperature at maximum exothermic heat flow during the cooling scan; X_c = weight percent crystallinity derived from the area under the melting endotherm (ΔH_f) and the heat of fusion of 100% crystalline pure sPS (ΔH_f°) according to the relationship $X_c = \dfrac{\Delta H_f}{\Delta H_f^\circ} \times 100\%$. Em dashes (—) indicate no thermal transition detected. All samples were heated to 300 °C and annealed for 3–5 min prior to cooling to erase thermal history.

the thermal properties and %X_c of the sPS homopolymer and the Random and Blocky samples after slow cooling (−10 °C min⁻¹) and 2 h isothermal crystallization at 190 °C. Consistent with findings of Genzer *et al.*,[45] the glass transition temperatures for both the Random and Blocky copolymers increase with degree of bromination, which is attributed to hindered rotations of the bulky *p*-bromostyrene units. For the Random copolymers, it is clear that the crystallizability is severely limited at degrees of bromination of 16% or more, in agreement with the work of Bae *et al.*[27] In contrast, the Blocky copolymers demonstrate a much greater aptitude for crystallization. For example, after isothermal crystallization at 190 °C, the Blocky B-21% yields a degree of crystallinity of X_c = 18% that constitutes 58% of the crystallinity of pure sPS, compared to only X_c = <1% for the lower Br-content Random R-18% sample. Again, the much greater crystallizability for the Blocky samples is strongly suggestive of a highly blocky microstructure.[23,27] For WAXD profiles of the sPS homopolymer and sPS-*co*-sPS-Br copolymers after isothermal crystallization, see Fig. S7.†

Crystallization kinetics

To investigate how the distribution of bromine defects along the chains affects the crystallization kinetics of the brominated copolymers, the Random and Blocky samples were subjected to isothermal crystallization at specific temperatures below T_m. To achieve rapid crystallization, chain segments of sufficient length, *i.e.*, stems, of uninterrupted styrene units are required to assemble into stable crystalline domains. Br-Sty monomers encountered at the crystal growth front are structural defects
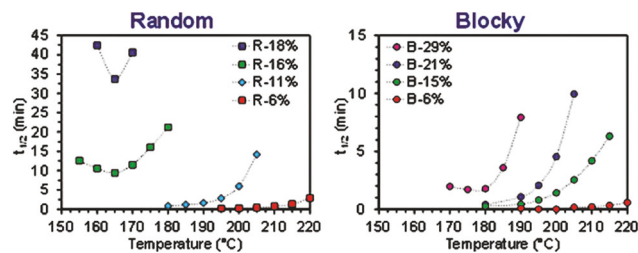

Fig. 5 Crystallization half-time ($t_{1/2}$) *versus* temperature profiles for the (left) Random and (right) Blocky copolymers. The $t_{1/2}$ scales are different to clearly demonstrate the rapid crystallization kinetics, small $t_{1/2}$ times, exhibited by the Blocky samples.

that are consequently excluded from attaching to the growing crystallite. This process of rejection of a defective stem and diffusion of a new stem to the melt-crystal interface ultimately slows the rate of crystallization. Fig. 5 shows the $t_{1/2}$ *versus* temperature profiles for the Random and Blocky copolymers. At approximately 6 mol% Br, both the Random and Blocky samples crystallize relatively fast; although, the Blocky B-6% sample exhibits shorter $t_{1/2}$ values than the Random R-6% (note the different *y*-axis scales). Above 6 mol% Br, the Blocky copolymers crystallize much faster, in under 15 min, and at lower supercooling compared to their Random analogs. For the highly brominated Blocky B-29% sample, the $t_{1/2}$ at 190 °C is 8 min. In contrast, the Random R-27% sample (not shown) was unable to crystallize during the isothermal crystallization experiments, even at high supercooling (2 h at 140 °C). These differences in crystallization kinetics between the Random and Blocky samples are attributed to the effect of microstructure on the probability of encountering a defective stem. As will be demonstrated below in the Simulations subsection, the blocky microstructure provides a greater prevalence of crystallizable segments (*i.e.*, runs of consecutive styrene units of sufficient length) along the polymer chains compared to the random microstructure. With more crystallizable stems, the blocky microstructure minimizes the time-consuming rejection/replacement process, and thus is capable of crystallizing in a shorter period of time.

Morphological characterization

USAXS/SAXS experiments were used to investigate the morphology of quenched films of the sPS-*co*-sPS-Br copolymers. The USAXS/SAXS profiles of the sPS homopolymer and the Random and Blocky copolymers are shown in Fig. 6. The scattering profiles of the Random copolymers are featureless with a q^{-4} dependence between 0.0004–0.004 nm⁻¹, which is consistent with the profile of the sPS homopolymer. In contrast, the Blocky copolymers exhibit excess scattering from a large-scale morphological feature at low q, between 0.0001–0.001 nm⁻¹. The Blocky B-29% sample also exhibits a second scattering feature at higher q, between 0.001–0.01 nm⁻¹. The dimensions of the features were determined using the Unified Fit model, summarized in Table S1.† The low q scattering feature, present only in the Blocky copoly-
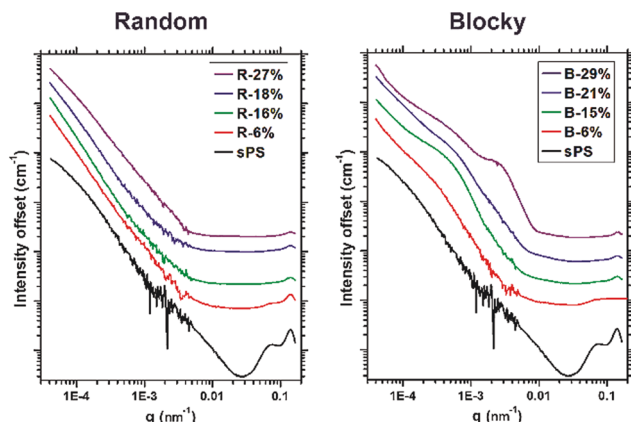
Fig. 6 USAXS/SAXS profiles of quenched films of the sPS homopolymer and the (left) Random and (right) Blocky copolymers. Films were prepared from powders of the homopolymer or copolymers by melt pressing between Kapton sheets at 30 °C above T_m for 20 s at 2200 psi then for 20 s at 4500 psi, followed by quenching in ice water to prevent sPS crystallization. For clarity, the scattering profiles and vertically offset.
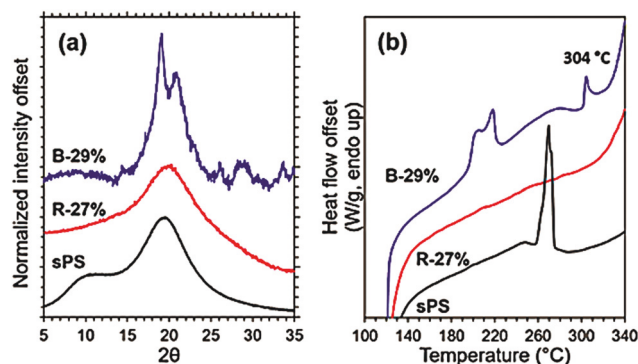

Fig. 7 (a) Wide-angle X-ray diffraction profiles of the melt-quenched Blocky B-29%, Random R-27%, and the sPS homopolymer samples, and (b) DSC heating scans of the Blocky B-29%, Random R-27%, and the sPS homopolymer samples following 1 h isothermal crystallization at 190 °C.

mers, fits to a dimension of *ca.* 30 nm and is consistent with a micro-phase separated morphology. The presence of this feature suggests that the "blockiness" originating from the gel-state functionalization is sufficient to drive phase development that is somewhat reminiscent of conventional block copolymer phase behavior. The physical and molecular origins of this large-scale feature observed in the USAXS profiles of the Blocky copolymers are attributed to a thermodynamic immiscibility between the electron-dense brominated sPS segments and the pure runs of sPS within the blocky microstructure of the functionalized chains.

The high q feature near $q = 0.002$ nm^{-1}, present only in the SAXS profile of the Blocky B-29% sample, fits to a dimension of 5.1 nm, which is surprisingly the same as the lamella thickness of semicrystalline sPS[46] (5.1 nm). However, since this sample was quenched from T_m + 30 °C (250 °C), it is not expected to contain crystalline sPS lamella. To investigate the origin of the high q scattering feature, the melt-quenched samples of Blocky B-29%, Random R-27%, and the sPS homopolymer were analyzed using WAXD. As expected, the WAXD data in Fig. 7(a) shows that the Random R-27% and the sPS homopolymer are completely amorphous. In distinct contrast, however, the Blocky B–29% sample exhibits a sharp crystalline reflection at 19.1° 2θ. It is important to note that this prominent reflection is not typically observed for melt-crystallized sPS.[47] Interestingly, the new prominent crystalline reflection at 19.1° 2θ, is similar to that previously observed in the diffractogram of an sPS copolymer that was polymerized with a high content (83 mol%) of *p*-chlorostyrene (19.4° 2θ), which was attributed to crystallization of the *p*-chlorostyrene units.[48] In addition, Guo *et al.*[34] reported that an sPS copolymer polymerized with a high content (59 mol%) of *p*-bromostyrene exhibits a high melting point of T_m = 317 °C, attributed to crystalline *p*-bromostyrene segments. In the DSC data for the Blocky

B-29% sample, Fig. 7(b), a distinct melting endotherm is observed at 304 °C. It is important to note that this melting endotherm is above the equilibrium melting point of pure sPS[47] and well above the temperature from which the WAXD and SAXS samples were quenched. Based on these WAXD and DSC data and the previous evidence of crystallization of halogenated sPS,[48] it appears that runs of Br-Sty units in the Blocky B-29% sample are capable of crystallizing even at this relatively low Br-content. While further analysis of this intriguing observation will be the subject for future investigations, these data strongly suggest that the gel-state bromination process is capable of producing a copolymer microstructure that can contain distinct sequences of Br-Sty units in segments of significant length. Consequently, we tentatively propose that the high q SAXS scattering feature observed in the melt quenched Blocky B-29% sample is attributed to the long period of crystalline Br-Sty segments.

Simulations of copolymer microstructure

To help rationalize the effect of copolymer microstructure on crystallization behavior after solution-state and gel-state functionalization, simulations of random and blocky copolymers were developed. The random microstructure resulting from homogeneous solution-state functionalization, is simulated by selecting monomers along a chain by random choice up to the desired degree of bromination. To simulate the blocky microstructure resulting from functionalization in the gel state, an inaccessible fraction of the total monomers in a chain is first established prior to random bromination of the remaining accessible fraction. Based on our hypothesis that the functionalizing reagent is sterically restricted to the solvent swollen amorphous chains within the semicrystalline gel, the inaccessible fraction of monomers is chosen to represent the fraction of monomers that are isolated within and in close proximity to the crystalline component of the gel network. From our XRD analysis (Fig. S8†), the degree of crystallinity, %X_c, of a 10 w/v% sPS/CCl$_4$ gel was determined to be 44%. In addition, it should also be recognized that chain seg-

ments in close proximity to the crystallites that emanate directly from the basal surfaces of the crystalline lamella may be locally restricted in their conformations (*i.e.*, a rigid amorphous fraction), which could also limit reagent accessibility. Based on the measurements of Cebe and coworkers,[49] the rigid amorphous fraction for sPS is estimated to be 11%. Thus, combining the measured %X_c of the gel with the estimated rigid amorphous fraction, our first approximation for the inaccessible fraction within the heterogeneous gel network is estimated (for the purposes of this preliminary simulation) to be 55%.

With the inaccessible fraction set, the blocky chain microstructure is constructed by first randomly selecting a monomer along the polymer chain of a given length (1442 monomer units long based on our sPS sample, M_w = 300 K; Đ = 2.0). Next, that monomer and its ±26 neighboring monomers are removed from the list of functionalizable monomers, resulting in an inaccessible block of 53 monomers. This chosen number of monomers in the inaccessible block is based on (1) an average lamellar thickness for solvent-crystallized sPS[46] of 5.1 nm; (2) the s(2/1)2 helical structure of the δ-form crystal structure of sPS[50] with 4 monomer units per identity period (*c*-axis dimension of the unit cell = 0.77 nm); and (3) the reasonable assumption that an attached stem has at least one fold. The process of selecting monomers for the inaccessible fraction is repeated until 55% of the monomers are marked inaccessible. Lastly, the remaining monomers within the accessible fraction are functionalized by random choice up to the desired degree of bromination.

For each degree of functionalization, the simulation generates 1000 polymer chains of 1442 monomers and calculates the frequency of a sequence length of j consecutive styrene units along each simulated chain. According to Flory's theory of crystallization in copolymers,[51] the probability (P_ζ) that a randomly selected styrene unit in the chain exists in a crystallizable chain segment of at least ζ styrene units is given by:

$$P_\zeta = \sum_j P_{\zeta,j} = \sum_{j=\zeta}^{\infty} \frac{(j - \zeta + 1) \times w_j}{j} \qquad (2)$$

where w_j is the probability that a unit chosen at random is a styrene unit in a sequence of length j, calculated by multiplying the mole fraction of styrene units (X_{Sty}) by the fraction of styrene units occurring in j sequences (j_{Sty}). For this work, ζ is defined as 26 monomer units, the average number of styrene monomers in one crystalline stem of an sPS crystallite.[10] (Note that the probability of consecutive brominated styrene units can also be computed. For an example, see Fig. S9).†

As shown in Fig. 8, the probability of selecting a crystallizable styrene monomer (*i.e.*, a monomer within a defect-free sequence of 26 monomer units) rapidly declines with increasing degree of bromination for the simulated random copolymers and falls below 1% at 18 mol% Br. This infrequency of crystallizable styrene monomers at 18 mol% Br is in excellent agreement with the experimentally-determined crystallizability of Random R-18%, which exhibits less than 1 wt% crystallinity
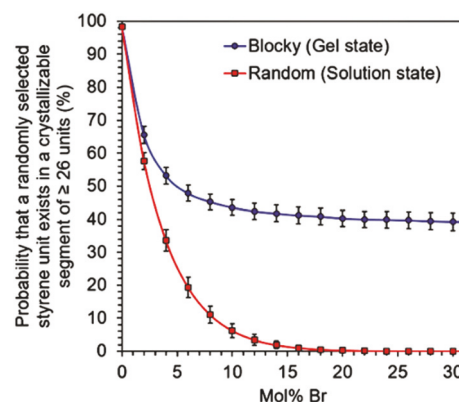

Fig. 8 Probability that a styrene unit selected at random exists in a crystallizable segment of at least 26 consecutive styrene units from simulations of theoretical blocky (gel-state) or random (solution-state) copolymers. Results based on 1000 polymer chains of 1442 monomer units. Error bars represent one standard deviation.

after 2 h isothermal crystallization at 190 °C (Table 1) and very slow crystallization at high supercooling (Fig. 5). Above 18 mol% Br, the probability of encountering a defect-free stem is very low, and thus the random copolymers are not predicted to be crystallizable. This prediction is in agreement with the amorphous nature of the Random R-31% sample; however, it is recognized that crystallization of styrene segments shorter than 26 units is possible, which is supported by the significant crystallizability (Table 1) observed in the Random R-16% sample.

In contrast to the predicted behavior of the random copolymers, the simulated blocky copolymers retain approximately 38% of their styrene monomers in crystallizable segments, even at 30 mol% Br. This result of the blocky simulation is in excellent agreement with the high crystallizability and rapid crystallization kinetics observed for the empirical Blocky copolymers. For example, the Blocky B-21% sample is capable of rapidly crystallizing ($t_{1/2}$ less than 2 min) to a degree of 18 wt% during isothermal crystallization at 190 °C. Thus, the agreement between these simulated copolymers and experiment validates the basis of our blocky copolymer simulation and confirms our hypothesis that restricting accessibility of the functionalizing reagent to monomers in the amorphous component of the gel network produces copolymers with a high prevalence of crystallizable homopolymer segments.

Another valuable outcome of these simulations is the ability to construct representative copolymer chain sequences for qualitative and quantitative comparison of the random and blocky microstructures. From the simulations, representative 29 mol% Br random and blocky copolymer chains were created, shown in Fig. 9. By inspection, it is clear that the simulated blocky 29 mol% Br copolymer exhibits longer segments of consecutive styrene units (open circles) compared to the simulated random copolymer. It is worth emphasizing that the distribution of these styrene "blocks" along the chain
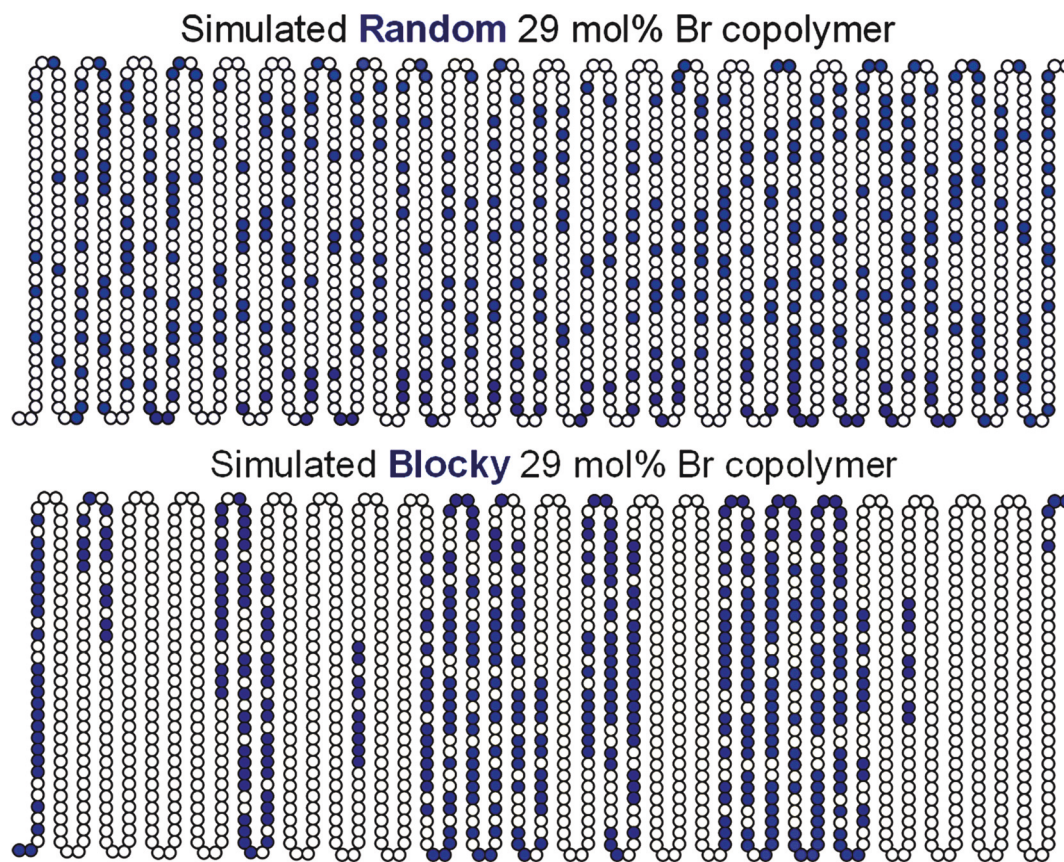
Simulated **Random** 29 mol% Br copolymer

Simulated **Blocky** 29 mol% Br copolymer

Fig. 9 Representative 29 mol% Br (top) random and (bottom) blocky copolymer chains derived from simulations. Each comonomer sequence is 1 of the 1000 copolymer chains of 1442 monomer units generated in the simulations. The particular sequence selected has a prevalence of pure styrene pentads (SSSSS, where S = styrene) that is most similar to the average number of SSSSS for all 1000 simulated chains. Open circles = styrene; filled circles = Br–Sty.

depends only on the position of the units that were randomly selected for the inaccessible fraction. For a quantitative comparison, the triad sequences can be counted along the simulated chains and grouped into one of the six possible unique triad combinations (*i.e.*, SSS, [SSB/BSS], BSB, SBS, [SBB/BBS], or BBB). The prevalence of encountering a given triad sequence is then calculated as a percentage of all unique triads counted along the simulated chains. For the simulated 29 mol% Br blocky copolymer shown in Fig. 9, this analysis yields a %BBB of 12% and %SSS of 57%. As noted above, the ^{13}C NMR results for the empirical Blocky B-29% sample yielded a BBB prevalence of 17% from spectral integration of the resonance at 143.1–143.3 ppm. Similarly, the SSS prevalence for this sample was measured by integration of the C(1) NMR spectrum at 144.8–145.4 ppm and found to be 57%. These empirical values are in good agreement with the values determined from the simulations, which further supports the validity of this simulation approach. An initial assessment of the difference between 12% (simulation) and 17% (empirical) for the BBB prevalence suggests that the empirical samples are more "blocky" than our preliminary model predicts. We are currently exploring a detailed analysis of the ^{13}C NMR results

from these copolymers aimed at developing a high-resolution sequencing protocol for further refinement of a microstructural model for blocky copolymers.

Conclusions

This work demonstrates the bromination of sPS in solution and in the heterogeneous gel state to produce random and blocky sPS-*co*-sPS-Br copolymers, respectively. The purpose of this research was to prepare semicrystalline blocky copolymers with relatively high degrees of functionality using a facile, post-polymerization functionalization method. Using our heterogeneous gel-state bromination method, a crystallizable 29 mol% Br sPS-*co*-sPS-Br copolymer was produced, demonstrating that this method favorably affects the bromination reaction to produce a blocky microstructure. When the brominating reagent is introduced into the heterogeneous gel network, it is excluded from the crystalline component and reacts with styrene monomers in the amorphous component. Based on the microstructural analysis of the Random and Blocky samples provided by NMR spectroscopy, gel-state bro-

mination produces sPS-*co*-sPS-Br copolymers with long segments of un-functionalized styrene "blocks" and segments of randomly functionalized "blocks" in a blocky microstructure. The USAXS/SAXS profiles of quenched films of the Blocky copolymers support that these distinct segments of pure sPS and randomly brominated sPS are capable of producing a micro-phase separated morphology attributed to thermodynamic immiscibility. The Blocky copolymers demonstrate superior crystallizability and faster crystallization kinetics at lower supercooling compared to their Random analogs. The microstructure of representative random and blocky copolymers generated from simulations of the homogeneous/heterogeneous bromination methods, affirms that restricting access of the functionalizing reagent to monomers well removed from the crystalline fraction of the gel network, produces copolymers with a greater prevalence of crystallizable sPS segments, which is advantageous for preserving desired crystallizability of the resulting blocky copolymers.

This work provides a fundamental investigation of the post-polymerization bromination of sPS, demonstrating that blocky sPS-*co*-sPS-Br copolymers can be prepared using a straightforward physical method of post-polymerization functionalization in the heterogeneous gel state. Given the high tactic purity and sequence specific ^{13}C NMR resonances, sPS is an ideal investigatory polymer for the gel-state functionalization reaction scheme. Future efforts will be focused on developing a deeper understanding of the relationship between gel morphology and the resulting copolymer microstructure in order to ultimately control the comonomer sequence distribution of sPS-*co*-sPS-Br copolymers. We anticipate that the dependence of sPS gel morphology on gelation solvent[7,8,52] will present avenues of further investigation into controlling the degree of blockiness in sPS-based copolymers. This research also lays the groundwork to synthesize other sPS-based blocky copolymers with useful functionalities through simple substitution of the labile bromine functional groups.

Conflicts of interest

There are no conflicts to declare.

Acknowledgements

Notes and references

1 N. Hadjichristidis, S. Pispas and G. A. Floudas, *Block Copolymers: Synthetic Strategies, Physical Properties, and Applications*, John Wiley and Sons, New York, 2002.

2 I. W. Hamley, *The Physics of Block Copolymers*, Oxford University Press, New York, 1998.

3 G. J. Domski, J. M. Rose, G. W. Coates, A. D. Bolig and M. Brookhart, *Prog. Polym. Sci.*, 2007, **32**, 30–92.

4 G. B. Fahs, S. D. Benson and R. B. Moore, *Macromolecules*, 2017, **50**, 2387–2396.

5 L. J. Anderson, X. Yuan, G. B. Fahs and R. B. Moore, *Macromolecules*, 2018, **51**, 6226–6237.

6 J. Mochizuki, T. Sano, T. Tokami and H. Itagaki, *Polymer*, 2015, **67**, 118–127.

7 H. Shimizu, T. Wakayama, R. Wada, M. Okabe and F. Tanaka, *Polym. J.*, 2005, **37**, 294–298.

8 M. Kobayashi, T. Yoshioka, T. Kozasa, K. Tashiro, J. Suzuki, S. Funahashi and Y. Izumi, *Macromolecules*, 1994, **27**, 1349–1354.

9 T. Roels, F. Deberdt and H. Berghmans, *Macromolecules*, 1994, **27**, 6216–6220.

10 C. Daniel, G. Guerra and P. Musto, *Macromolecules*, 2002, **35**, 2243–2251.

11 V. Venditto, M. Pellegrino, R. Califano, G. Guerra, C. Daniel, L. Ambrosio and A. Borriello, *ACS Appl. Mater. Interfaces*, 2015, **7**, 1318–1326.

12 S. D. Benson and R. B. Moore, *Polym. Prepr.*, 2009, **50**, 182.

13 S. D. Benson, Ph.D. Dissertation, Virginia Polytechnic Institute and State University, 2010.

14 A. Borriello, P. Agoretti, L. Ambrosio, G. Fasano, M. Pellegrino, V. Venditto and G. Guerra, *Chem. Mater.*, 2009, **21**, 3191–3196.

15 H. W. Gibson and F. C. Bailey, *Macromolecules*, 1980, **13**, 34–41.

16 J. J. Semler, Y. K. Jhon, A. Tonelli, M. Beevers, R. Krishnamoorti and J. Genzer, *Adv. Mater.*, 2007, **19**, 2877–2883.

17 Y. K. Jhon, J. J. Semler and J. Genzer, *Macromolecules*, 2008, **41**, 6719–6727.

18 L. A. Strickland, C. K. Hall and J. Genzer, *Macromolecules*, 2009, **42**, 9063–9071.

19 J. Han, B. H. Jeon, C. Y. Ryu, J. J. Semler, Y. K. Jhon and J. Genzer, *Macromol. Rapid Commun.*, 2009, **30**, 1543–1548.

20 Y. K. Jhon, J. J. Semler, J. Genzer, M. Beevers, O. A. Gus'kova, P. G. Khalatur and A. R. Khokhlov, *Macromolecules*, 2009, **42**, 2843–2853.

21 R. Gurarslan, S. Hardrict, D. Roy, C. Galvin, M. R. Hill, H. Gracz, B. S. Sumerlin, J. Genzer and A. Tonelli, *J. Polym. Sci., Part B: Polym. Phys.*, 2015, **53**, 155–166.

22 S. Liu and A. Sen, *Macromolecules*, 2000, **33**, 5106–5110.

23 Y. Gao and H. M. Li, *Polym. Int.*, 2004, **53**, 1436–1441.

24 R. A. Weiss, S. R. Turner and R. D. Lundberg, *J. Polym. Sci., Part A: Polym. Chem.*, 1985, **23**, 525–533.

25 R. A. Weiss, R. D. Lundberg and S. R. Turner, *J. Polym. Sci., Part A: Polym. Chem.*, 1985, **23**, 549–568.

26 L. Annunziata, Y. Sarazin, M. Duc and J. F. Carpentier, *Macromol. Rapid Commun.*, 2011, **32**, 751–757.

27 J. Shin, Y. Chang, T. L. T. Nguyen, S. K. Noh and C. Bae, *J. Polym. Sci., Part A: Polym. Chem.*, 2010, **48**, 4335–4343.

28 D. H. Howe, R. M. McDaniel and A. J. D. Magenau, *Macromolecules*, 2017, **50**, 8010–8018.

29 Q. Shen and J. F. Hartwig, *J. Am. Chem. Soc.*, 2006, **128**, 10028–10029.

30 J. Ilavsky, F. Zhang, R. N. Andrews, I. Kuzmenko, P. R. Jemian, L. E. Levine and A. J. Allen, *J. Appl. Crystallogr.*, 2018, **51**, 867–882.

31 J. Ilavsky, F. Zhang, A. J. Allen, L. E. Levine, P. R. Jemian and G. G. Long, *Metall. Mater. Trans. A*, 2013, **44**, 68–76.

32 J. Ilavsky, *J. Appl. Crystallogr.*, 2012, **45**, 324–328.

33 J. Ilavsky and P. R. Jemian, *J. Appl. Crystallogr.*, 2009, **42**, 347–353.

34 F. Guo, N. Jiao, L. Jiang, Y. Li and Z. Hou, *Macromolecules*, 2017, **50**, 8398–8405.

35 R. Gurarslan, A. Gurarslan and A. E. Tonelli, *J. Polym. Sci., Part B: Polym. Phys.*, 2015, **53**, 409–414.

36 S. N. Hardrict, R. Gurarslan, C. J. Galvin, H. Gracz, D. Roy, B. S. Sumerlin, J. Genzer and A. E. Tonelli, *J. Polym. Sci., Part B: Polym. Phys.*, 2013, **51**, 735–741.

37 R. Gurarslan and A. E. Tonelli, *Polymer*, 2016, **89**, 50–54.

38 J. C. Yang, M. J. Jablonsky and J. W. Mays, *Polymer*, 2002, **43**, 5125–5132.

39 L. C. Dickinson, R. Weiss and G. E. Wnek, *Macromolecules*, 2001, **34**, 3108–3110.

40 B. Chang, R. Zeigler and A. Hiltner, *Polym. Eng. Sci.*, 1988, **28**, 1167–1172.

41 Z. Wang, D. Liu and D. Cui, *Macromolecules*, 2016, **49**, 781–787.

42 D. Liu, M. Wang, Z. Wang, C. Wu, Y. Pan and D. Cui, *Angew. Chem.*, 2017, **129**, 2758–2763.

43 L. Annunziata, B. Monasse, P. Rizzo, G. Guerra, M. Duc and J.-F. Carpentier, *Mater. Chem. Phys.*, 2013, **141**, 891–902.

44 G. Gianotti and A. Valvassori, *Polymer*, 1990, **31**, 473–475.

45 A. E. Tonelli, Y. K. Jhon and J. Genzer, *Macromolecules*, 2010, **43**, 6912.

46 H. Wang, C. Wu, D. Cui and Y. Men, *Macromolecules*, 2018, **51**, 497–503.

47 E. M. Woo, Y. S. Sun and C. P. Yang, *Prog. Polym. Sci.*, 2001, **26**, 945–983.

48 A. D. Girolamo Del Mauro, F. Loffredo, V. Venditto, P. Longo and G. Guerra, *Macromolecules*, 2003, **36**, 7577–7584.

49 H. Xu, B. S. Ince and P. Cebe, *J. Polym. Sci., Part B: Polym. Phys.*, 2003, **41**, 3026–3036.

50 C. De Rosa, G. Guerra, V. Petraccone and B. Pirozzi, *Macromolecules*, 1997, **30**, 4147–4152.

51 P. J. Flory, *Trans. Faraday Soc.*, 1955, **51**, 848–857.

52 C. Daniel, A. Avallone and G. Guerra, *Macromolecules*, 2006, **39**, 7578–7582.